CFD SIMULATION OF HEAT TRANSFER OVER A SURFACE GROOVE

Institute of Engineering Thermophysics
National Academy of Sciences
Kiev, Ukraine

Kovalenko G. V. , Khalatov A. A., & Kobzar S. G.

Abstract

The PHOENICS v 3.5 software was employed to simulate numerically the local and average heat transfer over different grooves at turbulent flow. The freestream air velocity was change from 6.0 m/s to 60.0 m/s, providing the Reynold number range between 11,260 and 112,588. The trailing edge 'rounding-off', the 'smooth' entry, as well as the 'fencing of the groove sides leads to reduction in heat transfer. Two grooves arranged in-line enhance heat transfer, however this effect disappears at the high flow speed.

Keywords :

Heat transfer, groove, CFD simulation, augmentation.

Nomenclature

D - groove width, m; de - groove depth, m; f - relative increase in the heat exchange area due to the surface grooving; h, h_{pl} - average heat transfer coefficient: grooved surface, W(m^2K); Nu, Pr - Nusself and Prandtl number taken at the flow (air) temperature; Re - Reynolds number, based on the groove depth; Sh - Strouhal number, fD/U;U - air freestream velocity, m/s; X - axial distance from the channel inlet, m;Z - normal distance from the wall, m.

Introduction

Surface indentations in general and surface grooves in particular are widely used in several industrial applications. Typical examples are gas turbine cooling passages, heat exchangers, flow separation control over the round cylinder or over the airfoil. Within the groove or dimple the complex flow and heat transfer patter develops leading to the raise in heat transfer. The surface dimples enhance heat transfer; moreover, this enhancement exceeds the growth of associated pressure drop factor [1-3].

The optimistic assessments of the heat augmentation caused by indentations are well known. One of the earlier papers [4] has reported very high heat transfer augmentation rate (HTAR) factor of 6.3. However, the later study [5] has demonstrated much lower value of the HTAR. The HTAR factor of 2.5 associated with reduced pressure drop factor in the rectangular dimpled channel has been reported by Ligrani et al. [6]. A few factors affect the flow and heat transfer patterns within a dimple, the most important of them is the Reynolds number, freestream turbulence, the indentation geometry and configuration [7]. For spherical and cylindrical dimple, the heat transfer rate increases when the non-dimensional dimple depth de/D grows from 0 to 0.5 [7]. The second circulating flow in the deeper cylindrical dimple (de/D=1.49) leads to the blockage of heat transfer between freestream flow and the dimple bottom. Based on the published data analysis, Dreitser has concluded that the mechanism of heat transfer enhancement over a dimpled surface is identical to that reported for ribs, pins and fins [8]. Unlike this, many experimental data have demonstrated the non-trivial mechanism of heat transfer and fluid flow inside surface indentations.

Publications [11], [12] provide the magnitude of Reynolds number, where the surface dimples enhance heat transfer compared with the flat plate data. Starting from Re=2,500 the heat transfer begins to grow [11]; however at Re=350,000 the surface dimples no longer provide the growth of heat transfer [12]. Finally, the freestream turbulence reduces the surface dimples effect. The value of HTAR drops down due to effect of the freestream turbulence; finally, if it around 20% there is no difference between flat plate and surface dimple data [13]. Therefore, the external flow vorticity 'suppresses' the role of vortex structures bursting periodically out a dimple.

Objective

The current study is a numerical study of heat transfer on the grooved flat surface with the focus on the average data. Various cylindrically-shaped grooves arranged on the rectangular channel bottom surface were taken for consideration. The PHOENICS v 3.5 software was employed to predict numerically heat transfer at the flow conditions. The momentum and energy conservation equations were solved at the wall constant temperature. Following the convergence the grid size was designed using over 4,000 cells (143 in the X-direction; 28 in the Z-direction), the convergence was reached after about 6,000 iterations. The chosen turbulent closure was the RNG *k-e* turbulence model, providing the best results for flow with streamline curvature.

Test Cases

Overall 8 test cases have been calculated, all grooves were shaped by the round cylinder having 24.0 mm in a diameter. The groove width was 24.0 mm at all cases tested. The first groove configuration (No 1; Fig 1) is the 'pure' semi-cylinder with the non-dimensional depth (de/D) of 0.5. The other six grooves (No 1) had the cylindrically-shaped cross section with non-dimensional depth of 0.4; 0.29; 0.25; 0.168; 0.1; 0.05. The test case with two semi-cylindrical grooves arranged in-line (one after another) was also studied (No 5). The axial distance between groove centers was taken as 43.2 mm.

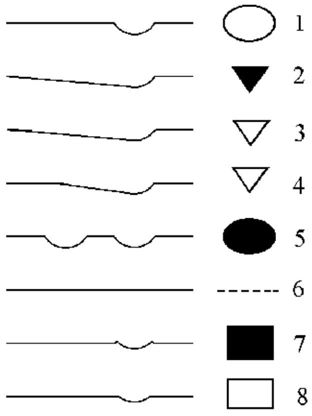

Figure 1 Surface groove configurations.

Three cases with 'smooth' inlet have been considered providing the plane slope towards the groove bottom. This slope is 6.8 degrees for the test case No 2 and 20.5 degrees - for the case No 4. Unlike the case No 2, the 'rounded off' trailing edge (radius: 1mm) was configured in the case No 3 (slope: 6.8°) to reduce the overall pressure losses. The test No 8 (de/D=0.29) was also introduced to investigate the role of small semi-cylindrical 'fences' (height and radius: 1.2 mm) in-front and after the single groove. This test was compared with the same single groove (de/D=0.29), but without fences (No 7). The flat plate case (No 6) was also calculated as a baseline configuration for further comparisons.

The groove to be calculated was placed on the rectangular channel bottom having 278 mm long and 82 mm height. The groove leading edge is 88.0 mm from the channel entrance. The entry air velocity was ranged from 6.0 m/s to 60.0 m/s, providing the Reynolds number Re between 11,260 and 112,588. This boundary layer thickness in-front of the groove was 2.03 mm (V=6.0m/s), 1.06 mm (V=22.0 m/s), and 0.64mm (V=60.0 m/s).

The heat transfer coefficient was averaged using two axial 'boundaries' - 20.0 mm upstream and 48.0 mm downstream of the groove.

Results and Discussions

The contours of axial velocity inside the semi-cylindrical groove can be seen from the Fig 2. The Flow direction is from the left to the right, the freestream air temperature is 20°C, the wall temperature is 0°C. The in-groove flow structure is fairly complex; the flow velocity is low near the groove bottom, while the increased velocities are around the groove trailing edge and over the flat surface following the groove.

Figure 3 demonstrates the local heat transfer over the grooved surface (U=22.0 m/s for the variable groove depth. The heat transfer over the flat plate is also given for comparison. In front and immediately after the groove, the local heat transfer co-efficient is higher, while inside groove is lower than that for the flat plate data. As the groove becomes deeper, the heat transfer in-front and after the groove increased, while inside the groove reduces. The latter is due to the low velocity level near the groove bottom area.

Figure 2 Contours of axial velocity inside the semi-cylindrical groove (de/D=0.5).
U = 22.0 m/s, Re = 41,282

Figure 3 Local heat transfer over the grooved wall; effect of the groove depth.
Dotted line : flat plate

Figure 4 Heat transfer ratio; effect of the groove depth.

The average heat transfer (Fig 4) reflects the opposite influence of groove depth on heat transfer. At the lower velocity (U=22.0 m/s) the resulting curve is close to the unity for the de/D ratio between 0.1 and 0.4. At the higher velocity (U=60.0 m/s) the heat transfer reduction inside the groove prevails; as a result the resulting curve is lower than the unity for the entire range of de/D ratio. For both velocities, the minimum heat transfer h/h_{p1} ratio locates between 0.15 and 0.25.

Actually, the flow field inside the groove is unsteady with the bulk flow oscillations bursting out of groove. The limited time-dependant calculations inside the groove with de/D=0.44 has been made at the freestream velocity of 6.0 m/s (Re=11,258). The processing of data has provided the frequency of fluctuations out of groove. The associated Strouhal number Sh is 0.04, that is quite close to the Strouhal number measured over the flat plate with a single hemispherical dimple [13].

The Figure 5 represents the average heat transfer data over a grooved surface. For single grooves the heat transfer exceeds the flat plate data in the region between 18.0 m/s and 32.0 m/s. The best results demonstrates the groove No 1, the worst data was obtained for the groove No 7. Both the trailing edge 'rounding-off' , as well as the groove 'fencing' (No 7) reduce the heat transfer. The best results at low velocity demonstrates the double groove (No 5), where the heat transfer ratio is over factor of 4.0 at U=10.0 m/s. Nevertheless, the effect of double grooving drops down at the air velocity growth and becomes lower the flat plate data at U>50.0 m/s. Apparently, it is due to the short distance between grooves leading to 'loosing' of enhanced area after the first groove. That is why the 'double-grooved' curve (No 5) reduces with the air speed growth, while all other curves (single grooves) increase.

Figure 5 Average heat transfer over the grooved wall. (related to the smooth surface area). *Dotted line* : smooth surface *Legends* : Figure 1

Figure 6 Average heat transfer over the grooved wall. (related to the overall heat exchange area). *Dotted line*; smooth surface. *Legends* : Figure 1

If the overall heat exchange area (including the groove surface) is taken into consideration (Fig 6), then the region of advantageous application of single grooves is between 17.0 m/s and 21.0 m/s, while the same area for the double-grooved locates below 39.0 m/s. As before, at U<21.0 m/s the best results demonstrates the groove No 1, however the shallower dimple No 8 becomes the best one at U=60.0 m/s.

The Surface groove generates primarily the two-dimensional (X-Z) flow field. The limited calculations were made for the single dimple, generating the three-dimensional flow field. The spherically-shaped dimple had the surface diameter of 24.0 mm and the depth of 7.0 mm (de/D=0.29). Compared with the groove No 8, this dimple has provided the average heat transfer around 90% higher over the same heat exchange area.

Conclusions

The CFD heat transfer simulation over the cylindrically-shaped grooves has been carried out at the turbulent flow conditions. Despite the groove enhances local heat transfer in-front and after the groove, the average heat transfer can be higher and lower of the flat plate data depending on the freestream velocity. This is due to the relatively low flow velocity and associated heat transfer near the groove bottom. The 'rounding-off' of the trailing edge and especially the groove 'fencing' reduces the heat transfer. As found, the single dimple provides the higher heat transfer rate at identical geometry and flow conditions. The further pressure drop calculations should be established to assess the thermal-hydraulic performance of the investigated groove configurations.

Acknowledgement

This research was partly funded by the International CRDF Grant no. UE2-552-KV-02. Only the author's conclusions are given in this paper.

References

1. Kiknadze G I & Oleinikov V G . The self-organisation of the tornado-like vortex structures in gas and liquid flow and heat and mass transfer enhancement. (In Russian) – Novosibirsk: Preprint No 227-90, *Institute of Thermophisics of Siberian Branch of the Academy of Sciences of USSR* (Publishers) 1990 – 45pp.
2. Aleksandrow A A, Gorelov G M , Danil’chenko V P & Reznik V E . Heat transfer and hydraulic resistance under the flow of surface with the developed roughness in the manner of the spherical deepenings. (In Russian) // *Promyshlennaya Teplotehnika* 1989 **11** No 6 – Pp 56-63.
3. Afanas’ev V N , Leont’ev A I & Chudnovsky Ya P. The heat transfer and friction on surfaces shaped by the spherical depressions. (In Russian) – Moscow : *The Publishing Company MGTU* 1990 – 118pp
4. Chapman D R , A Theoretical analysis of heat transfer in regions of separated flow, *NACA TN 3792,* Oct 1956
5. Hagen R L & Danak A Mm Heat transfer in the field of the turbulent boundary layer separation over a dimple. // *Heat Transfer* 1967 No 4 – Pp 62-69
6. Mahmood G I, Hill M L, Nelson D L, Ligrani P M, Moon H K & Glezer B. Local heat transfer and flow structure on and above a dimpled surface in a channel. //*Proceedings of ASME TURBO EXPO 2000*, May 8-11 2000, Munich Germany #2000-GT-230.
7. Leont’ev A I< Olimpiev V V, Dilevskaya E V & Isaev S A. The nature and mechanism of the heat transfer enhancement on the surface structured with spherical cavities. (In Russian) //*Reports of the Russian Academy of Sciences,* Ser. Energy and Power Systems, 2002, No 2 Pp 117-133.
8. Dreitser G A The modern status of the heat transfer enhancement studies in a channel and prospects of a compact heat exchanger design. (In Russian) //*Heat and Mass Transfer,* MIF-96, Minsk 1996 **10** Part 1 Pp 26-39.
9. Terekhov V I, Kalinina S V & Mshvidobadze Ju. M. Heat transfer over the spherically-shaped cavity located on the rectangular channel wall. (In Russian) // *Teplofizika Visokih Temperatur* 1994 **32** No 2 Pp 249-254.
10. East L F Aerodynamic induced resonance in rectangular cavities. //*Journal of Sound and Vibrations* 1966 **3** Pp 277-287
11. Presser K H Empirische gleichungen zur berechnung der stoff – und warmeubertragung fur den spezialfal der abgerissenen stromung // *Int. J Heat Mass Transfer* 1972 **15** Pp 2447-2471.
12. Borovoy V Ya & Jakovlev L V Heat transfer under a supersonic flow over a single dimple (In Russian) // *Mechanika Zidkosti I Gaza* 1991 No 5 Pp 48-52.
13. Kesarev V S & Kozlov A P. The flow structure and heat transfer over the hemispherical depression at the turbulent air overflow. (In Russian) // *Bulletin of MGTU,* Ser. Mashinostroenie 1993. No 1 Pp 106-115.